Reprinted from Journal of the Optical Society of America B, Vol. 4, page 882, June 1987

Degenerate stimulated parametric scattering in $LiNbO_3$:Fe

G. Zhang,* Q. X. Li,† P. P. Ho, and R. R. Alfano

Institute for Ultrafast Spectroscopy and Lasers, Departments of Physics and Electrical Engineering, The City College of New York, New York, New York 10031

S. Liu and Z. Wu

Department of Physics, Nankai University, Tianjin, China

Received May 16, 1986; accepted December 5, 1986

Nonlinear photoinduced light scattering at 414 nm in $LiNbO_3$:Fe caused by degenerate stimulated parametric scattering and its competition process with the photorefractive noise phase gratings have been observed. The phase-matching scattered light was located in a plane normal to the polar axis of crystal.

Over the years several forms of photoinduced light scattering have been observed from a $LiNbO_3$:Fe crystal illuminated by a coherent light beam.[1–7] Owing to the anisotropy of the $LiNbO_3$ crystal, the scattering pattern depends both on the propagation direction of the light beam relative to the crystallographic axes and on the beam polarization. Most studies have been performed for isotropic photoinduced scattering of extraordinary waves.[1,2,7] When an ordinary wave is incident, a small-angle-spread extraordinary-wave light scattering, polarized perpendicular to the crystal optic axis, is observed.[3,5,6] It has been suggested[5] that the change in photoinduced light scattering with orthogonal polarization that arises from the recording of the photorefractive noise phase grating (PNPG) as a result of the excitation of a specific spatially oscillating photovoltaic current in the crystal. For example, degenerate stimulated parametric scattering (DSPS) in $LiTaO_3$:Cu was recently observed by Odoulov *et al.*[8] The scattered light was located in a ring pattern with the apex angle defined by the phase-matching condition of the forward four-wave mixing of ordinary and extraordinary light through the crystal photovoltaic current. Temple and Warde[4] sent an extraordinary polarized wave through $BaTiO_3$ and $LiNbO_3$:Fe crystals and observed a well-defined scattered ring pattern of ordinary polarized light. Here we report on the observation of *strong* four-wave DSPS in a $LiNbO_3$:Fe crystal at a well-defined angle using ordinary polarized light at 414 nm and its relative competition process with the PNPG.

The experimental arrangement is shown in Fig. 1. An ordinary polarized krypton-ion laser beam at 414 nm illuminated X- or Y-cut samples of $LiNbO_3$:Fe crystal (0.08 wt. %). The spot size and the power of the incident laser beam were adjustable parameters in the experiment. Two types of extraordinary-wave photoinduced scattering pattern were observed by using an ordinary incident wave under various conditions. One type of scattered light was the small-angle light scattering (PNPG) with an angular spread from 2° to 20°. This type of scattering was previously observed by illuminating the crystal with a helium–cadmium laser beam ($\lambda = 441.6$ nm) or an argon-ion laser beam ($\lambda = 488.0$ nm or $\lambda = 514.5$ nm).[3,5,6] The second type of photoinduced scattering, which is a new type, occurs at a higher power level and is located at a larger scattering angle spread from 44° to 49°. We did not observe large-angle light scattering when we used an argon-ion laser beam operating at $\lambda = 488.0$ or 514.5 nm even with a larger power level of about 1 W. When a 414-nm laser is used, depending on the illumination beam intensity and the beam size in the crystal, both types of the photoinduced scattering compete for dominance.

It took a long time to develop the large-angle light scattering pattern in comparison to the formation of small-angle light scattering. At first, scattered light with the form of an ordinary wave in the plane containing the propagation direction of the incident beam and the polar axis of the crystal was observed. After a few seconds, the length of time depending on the illumination beam power, the intensity of the ordinary-wave scattering gradually decreased, and the large-angle or the small-angle extraordinary-wave scattering intensity was increased, finally reaching a saturation level. The induced grating for the extraordinary-wave scattering can be stored in the crystal for several days.

In Fig. 2 the intensity dependence of both types of photoinduced scattering pattern, PNPG and DSPS, is displayed. These photographs of scattering patterns were taken by illuminating the crystal with a krypton-ion laser beam at different power levels. In Fig. 2(a) the incident laser power was set at 100 mW, and only the small-angle scattering pattern (PNPG) occurred. As the laser power was increased to 200 mW, large-angle scattering (DSPS) appeared. In Fig. 2(b) the intensity distributions of both types of scattering pattern are similar. When the laser power was increased to 300 mW, the large-angle scattering (DSPS) became stronger and the small-angle scattering (PNPG) disappeared. After the laser power was decreased, the competitive process reversed. It is clear that the larger power of the illumination beam is more favorable to DSPS.

The competition process of PNPG and DSPS as a function of the illuminating beam size is displayed in Fig. 3. In both parts of Fig. 3, the incident laser power was 300 mW. The illumination beam sizes were 0.4 and 0.7 mm in Figs. 3(a) and 3(b), respectively. The illumination intensity of a small spot size in Fig. 3(a) was three times stronger than that

0740-3224/87/060882-04$02.00

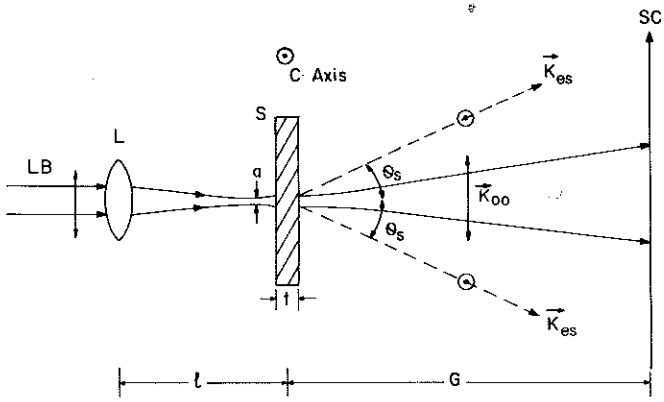

Fig. 1. Experimental arrangement. LB, 414-nm krypton laser; L, lens; t, thickness of sample (= 1 mm); *l*, distance from lens to sample [= 3.5 cm for Figs. 2 and 3(a) and 3.4 cm for Fig. 3(b)]; G, distance from sample to film screen; SC, photographic film; $\mathbf{K}_{es}$, DSPS scattering wave vector. The incident laser is an ordinary polarized wave with respect to the sample.

in Fig. 3(b). It is clear that a larger illumination beam size is more favorable to DSPS.

In addition, when the illuminating beam size in crystal was very small, for example, $a = 12\ \mu$m, where the calculated fringe spacing of the phase grating is 50 μm,[7] neither DSPS nor PNPG was induced. In this extreme case, the power density of the laser beam in the crystal was thousands of times greater than that for $a = 0.7$ mm, where the calculated grating space is $\sim 1\ \mu$m.[7] Therefore, the illumination beam size must be greater than the induced grating period.

Small-angle light scattering is due to the recording of PNPG's by the excitation of specific spatially oscillating photovoltaic current in a $LiNbO_3$:Fe crystal.[5] The large-angle light scattering in a $LiNbO_3$:Fe crystal is similar to the nonlinear light scattering in a $LiTaO_3$:Cu crystal caused by degenerate stimulated forward four-wave mixing of waves with orthogonal polarizations.[8] The uniqueness of the narrow-scattering angular window of DSPS indicates the necessity for the phase-matching condition.

In Fig. 4, a vector diagram for the formation of a new DSPS process is presented. Figure 4(a) displays a model for the formation of the initial weak-noise phase gratings (PNPG's) in a crystal[7] due to the interference of the incident beam $\mathbf{K}_{oo}$ with weak scattered beams $\mathbf{K}_{os}^{(1)}$, $\mathbf{K}_{os}^{(2)}$, $\mathbf{K}_{os}^{(3)}$, ... originating from imperfections in crystal, where $\mathbf{K}_{oo}$, $\mathbf{K}_{os}^{(1)}$, $\mathbf{K}_{os}^{(2)}$, $\mathbf{K}_{os}^{(3)}$, ... represent the ordinary wave vectors of the incident beam and the scattered beams. Vectors $\mathbf{K}_g^{(i)}$ are defined as the recorded noise phase-grating vectors $\mathbf{K}_{os}^{(i)} - \mathbf{K}_{oo}$, where $i = 1, 2, \ldots, N$. The scattered waves and the incident wave are coupled off these gratings. They all terminate at a sphere surface S with its radius equal to $|\mathbf{K}_{oo}| = n_o(2\pi/\lambda)$, where n_o is the ordinary refractive index of the crystal.

In Fig. 4(b), when one of these noise phase gratings in Fig. 4(a) has met the phase-matching condition, the orthogonal polarization scattering occurs through four-wave mixing, where $\mathbf{K}_{es}$ is the wave vector of the extraordinary scattered wave and $\mathbf{K}_g = \mathbf{K}_{oo} - \mathbf{K}_{os}$ is the phase-matching grating vector. An alternative method for the four-wave mixing process is shown in Fig. 4(c), with the dashed lines corresponding to the vectors in Fig. 4(b). This four-wave mixing process of orthogonal polarization waves, $2\mathbf{K}_{oo}$ and $2\mathbf{K}_{es}$, in turn increases the amplitude of the phase-matching grating because of the standard photorefractive origin ($\delta\chi_{13}$, $\delta\chi_{31}$, $\delta\chi_{23}$, and $\delta\chi_{32}$ are nonzero).[4] This process will continue to amplify the formation of the phase-matching grating. The amplitude of the phase-matching grating increases more when the waves used in this four-wave mixing process have orthogonal polarization. Therefore the extraordinary-wave scattering at a well-defined scattering angle gradually increases until it is saturated. Owing to the termination of $\mathbf{K}_g$ at the sphere surface S, as illustrated by the dahsed lines in

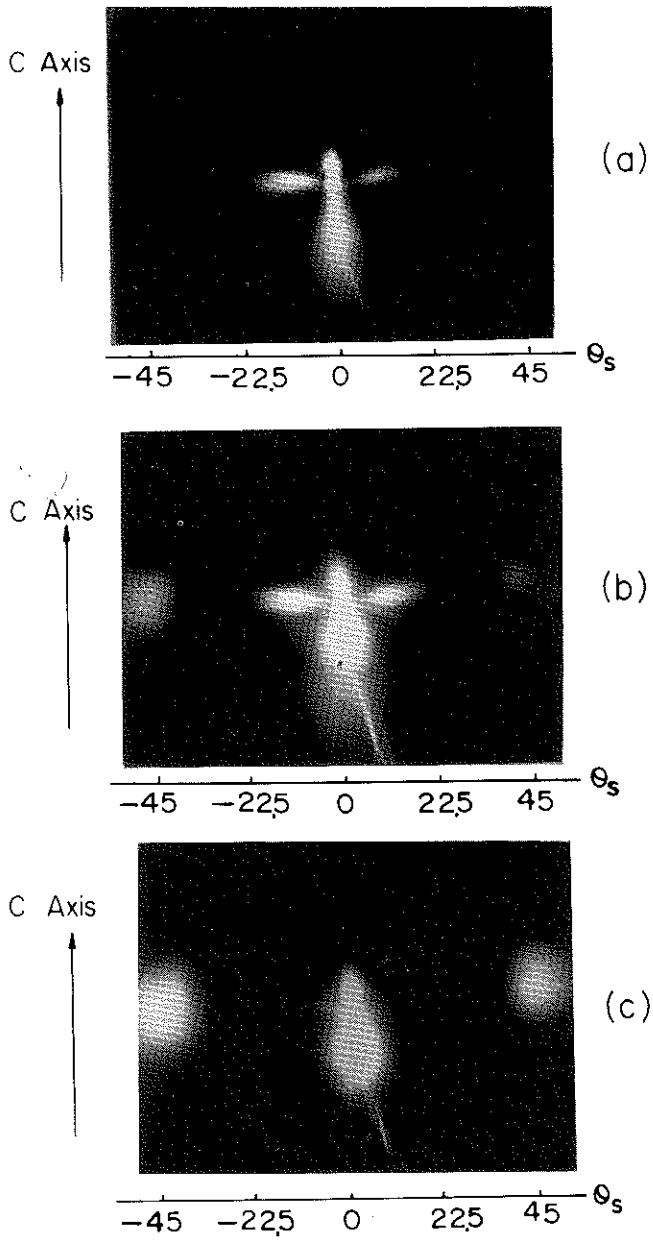

Fig. 2. Photographs of the incident laser intensity dependence of the competitive process between the ordinary scattering PNPG and DSPS. The horizontal axis represents the scattering angle θ_s. The beam spot size at sample is about 0.4 mm. The optic axis is marked by an arrow at the left. (a) $P_{in} = 100$ mW, (b) $P_{in} = 200$ mW, (c) $P_{in} = 300$ mW. The middle (up–down) scattering in each photograph is ordinary PNPG. The 2°–20° side scattering in (a) and (b) is extraordinary PNPG. In (c) the new scattering (DSPS) at $\theta_S \sim 45°$ is observed. The experimental error was ±1°.

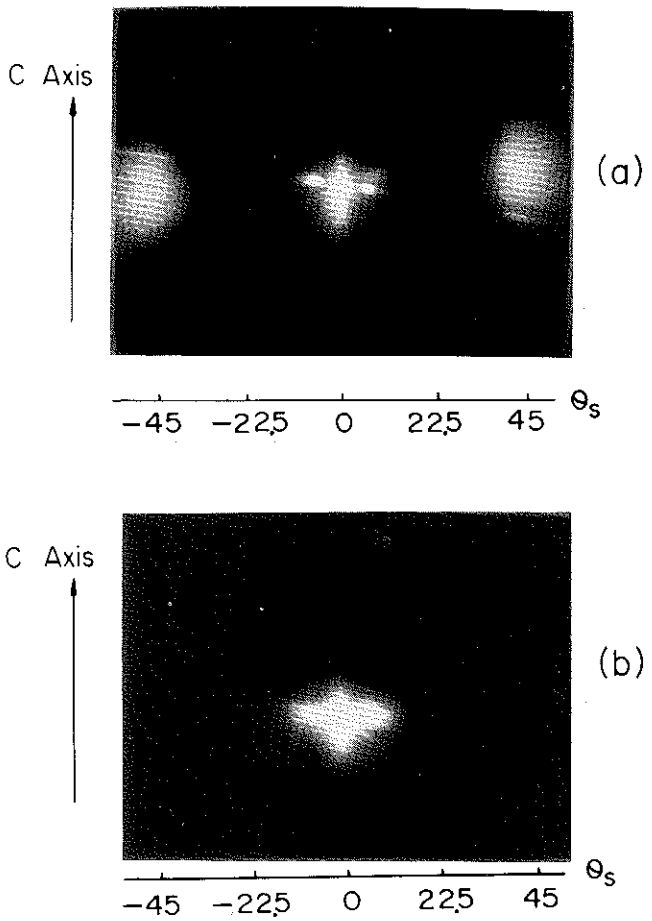

Fig. 3. Photographs of the induced scattering as a function of the incident laser-beam spot size: (a) $a = 0.4$ mm, (b) $a = 0.7$ mm. The incident laser power was maintained at 300 mW for both cases. In (b) the spot size increased and the intensity decreased; however, DSPS increased.

Fig. 4(b), the phase-matching condition of the vectors $\mathbf{K}_g$, $2\mathbf{K}_{oo}$, and $2\mathbf{K}_{es}$ constitutes a right triangle. From this vector relationship, the scattering angle is

$$\theta_s = \sin^{-1}[(n_e/n_o(n_o^2 - n_e^2)^{1/2}]. \quad (1)$$

This equation is derived in Appendix A.

Using $n_o = 2.4223$ and $n_e = 2.3103$ at $\lambda = 414$ nm,[9] in Eq. (1), the calculated scattering angle $\theta_s = 44°$. This theoretical calculation agrees well with the experimental result.

The wavelength dependence of the DSPS may originate from the amplification process of the phase-matching grating. Because of the absorption[1] of the iron impurities at 414-nm wavelength excitation, a large number of photoexcited carriers from the band-to-band tail transitions are trapped to form a photorefractive phase-matching grating with a larger amplitude. As long as the absorption is not too large, the gain of the phase-matching grating amplification prefers the shorter-wavelength light excitation. At 488- or 514-nm wavelength excitation, the absorption by this crystal is significantly less. This may be the reason why DSPS was not observed at longer wavelengths.

In conclusion, PNPG- and DSPS-induced scattering in a $LiNbO_3$:Fe crystal was observed and analyzed. The competition between the large-angle light scattering (DSPS) and the small-angle light scattering (PNPG) indicates different generation mechanisms for these two processes. The large-angle light scattering depends more on the wavelength, the spot size, and the intensity of the illumination beam. This illumination beam intensity-dependent competition process has been applied to analyze light scattering. In addition, large-angle extraordinary-wave light scattering (DSPS) requires a phase grating with a larger vector. In order to obtain such phase matching, a larger illumination beam spot size in crystal is required.[7] These effects could be used for optical logic devices.

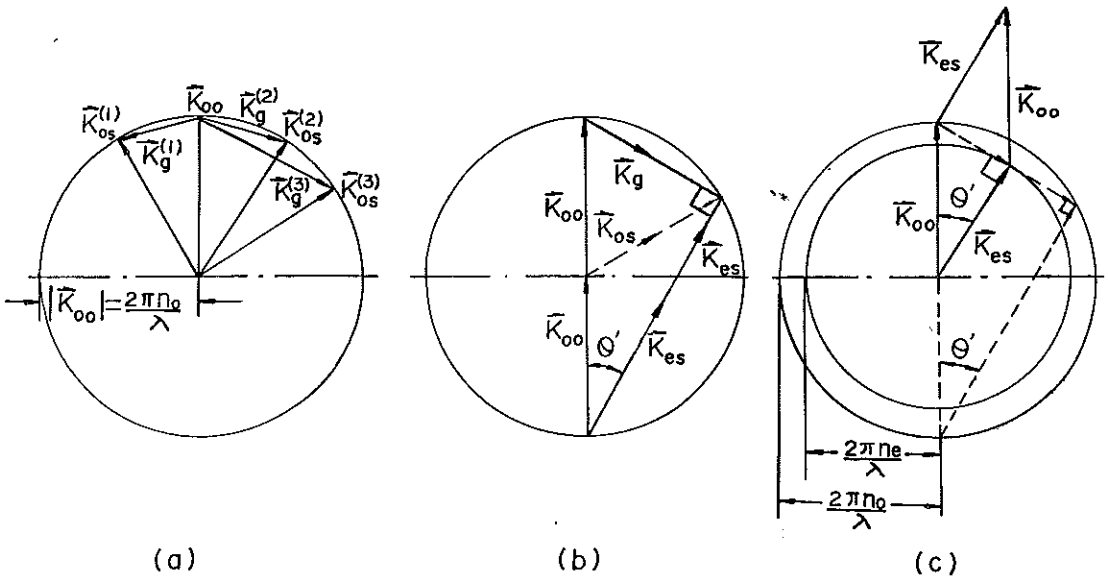

Fig. 4. Hypothetical vector diagrams of DSPS-induced light scattering. (a) Formation of noise phase grating $\mathbf{K}_g^{(i)}$. (b) Phase-matching condition of DSPS: $\mathbf{K}_g$ and $2\mathbf{K}_{es}$, which form the short axes of a triangle on a semicircle using the diameter as the base, must be perpendicular to each other. (c) Alternative expression of four-wave mixing of (b) ($n_e < n_o$). $\mathbf{K}_{oo}$, incident laser wave vector $(=2\pi n_o/\lambda)\hat{K}$. $\mathbf{K}_g^{(i)}$, ith component of the phase grating vector $[=\mathbf{K}_{os}^{(i)} - \mathbf{K}_{oo}]$. $\mathbf{K}_{os}$, weak ordinary scattered wave vector of the ith component originating from crystal imperfections. $\mathbf{K}_g$, phase-matching grating vector of DSPS. $\mathbf{K}_{es}$, extraordinary scattered wave vector.

APPENDIX A: DERIVATION OF EQ. (1)

From the phase matching required for the right-triangle configuration in Fig. 4(b), we obtain

$$\sin\theta' = |\mathbf{K}_g|/2|\mathbf{K}_{oo}|, \tag{A1}$$

where θ' is the DSPS scattered angle in crystal. Since

$$|\mathbf{K}_{oo'}| = (2\pi/\lambda)n_e, \tag{A2}$$

$$|\mathbf{K}_{os}| = (2\pi/\lambda)n_e, \tag{A3}$$

we have

$$|\mathbf{K}_g| = (|2\mathbf{K}_{oo}|^2 - |2\mathbf{K}_{es}|^2)^{1/2} = (4\pi/\lambda)(n_o^2 - n_e^2)^{1/2}. \tag{A4}$$

Combining Eqs. (A1), (A2), and (A4), we obtain

$$\sin\theta' = (n_o^2 - n_e^2)^{1/2}/n_o. \tag{A5}$$

The DSPS scattered angle in air, θ_S, can be obtained from the DSPS scattered angle in the crystal, θ', by using Eq. (A5) and the following kinematic relation:

$$\theta_S = \sin^{-1}(n_e \sin\theta') = \sin^{-1}[(n_e/n_o)(n_o^2 - n_e^2)^{1/2}]. \tag{1}$$

ACKNOWLEDGMENTS

This research is supported in part by U.S. Air Force Office of Scientific Research grant 84-0144 and by grants from the National Science Foundation and the Professional Staff Congress/Board of Education.

* Visiting Senior Scholar (American Physical Society–People's Republic of China Visitors Program); permanent address, Department of Physics, Nankai University, Tianjin, China.

† Permanent address, Department of Physics, Zhongshan University, Canton, China.

REFERENCES AND NOTES

1. W. Phillips, J. J. Amodei, and D. L. Staehler, RCA Rev. **33,** 94 (1972).
2. R. Magnussen and T. Gaylord, Appl. Opt. **13,** 1545 (1974).
3. E. M. Avakyan, S. A. Alaverdyan, D. G. Belabaev, V. K. Sarkisov, and D. M. Tumanyan, Sov. Phys. Solid State **20,** 1401 (1978).
4. D. A. Temple and C. Warde, J. Opt. Soc. Am. B **3,** 337 (1986).
5. E. M. Avakyan, K. G. Belabaev, and S. G. Odulov, Sov. Phys. Solid State **25,** 1980 (1983).
6. S. Liu, G. Zhang, Z. Wu, G. Li, S. Feng, J. Zhang, J. Zhao, and L. Xu, Acta Phys. Sin. **33,** 105 (1984) [Chin. Phys. **4,** 593 (1984)].
7. G. Zhang, Q. X. Li, P. Ho, R. Alfano, S. Liu, and Z. Wu, Appl. Opt. **25,** 2955 (1986).
8. S. Odoulov, K. Belabaev, and Z. Kiseleva, Opt. Lett. **10,** 31 (1985).
9. n_o and n_e at $\lambda = 414$ nm are calculated by the following formulas:

$$n_o = 1 + \frac{1.1932\lambda^2}{\lambda^2 - 0.0276(\mu m)^2}, \qquad n_e = 1 + \frac{1.1183\lambda^2}{\lambda^2 - 0.0251(\mu m)^2}.$$

   The numerical values were obtained by using the values of the refractive index at $\lambda = 420$ nm and $\lambda = 450$ nm.[10]
10. G. D. Boyd, W. L. Bond, and H. L. Carter, J. Appl. Phys. **38,** 1941 (1967).